

1 Measurement report: Emissions of intermediate-volatility organic compounds from
2 vehicles under real-world driving conditions in an urban tunnel

3 Hua Fang^{1,2,4}, Xiaoqing Huang^{1,2,4}, Yanli Zhang^{1,2,3*}, Chenglei Pei^{1,4,5}, Zuzhao Huang⁶, Yujun Wang⁵,
4 Yanning Chen⁵, Jianhong Yan⁷, Jianqiang Zeng^{1,2,4}, Shaoxuan Xiao^{1,2,4}, Shilu Luo^{1,2,4}, Sheng Li^{1,2,4}, Jun
5 Wang^{1,2,4}, Ming Zhu^{1,2,4}, Xuwei Fu^{1,2,4}, Zhenfeng Wu^{1,2,4}, Runqi Zhang^{1,2,4}, Wei Song^{1,2}, Guohua
6 Zhang^{1,2}, Weiwei Hu^{1,2}, Mingjin Tang^{1,2}, Xiang Ding^{1,2}, Xinhui Bi^{1,2}, Xinming Wang^{1,2,3,4*}

7

8 ¹State Key Laboratory of Organic Geochemistry and Guangdong Key Laboratory of
9 Environmental Protection and Resources Utilization, Guangzhou Institute of Geochemistry,
10 Chinese Academy of Sciences, Guangzhou 510640, China

11 ²CAS Center for Excellence in Deep Earth Science, Guangzhou, 510640, China

12 ³Center for Excellence in Urban Atmospheric Environment, Institute of Urban Environment,
13 Chinese Academy of Sciences, Xiamen 361021, China

14 ⁴University of Chinese Academy of Sciences, Beijing 100049, China

15 ⁵Guangzhou Ecological and Environmental Monitoring Center of Guangdong Province,
16 Guangzhou 510060, China

17 ⁶Guangzhou Environmental Technology Center, Guangzhou 510180, China

18 ⁷Guangzhou Tunnel Development Company, Guangzhou 510133, China

19

20 *Correspondence to: Dr. Xinming Wang (e-mail: wangxm@gig.ac.cn) and Dr. Yanli Zhang (e-
21 mail: zhang_y186@gig.ac.cn)

22

23 **Abstract**

24 Intermediate-volatility organic compounds (IVOCs) emitted from vehicles are important
25 precursors to secondary organic aerosols (SOA) in urban areas, yet vehicular emission of
26 IVOCs, particularly from on-road fleets, is poorly understood. Here we initiated a field
27 campaign to collect IVOCs with sorption tubes at both the inlet and the outlet in a busy urban
28 tunnel (>30,000 vehicles per day) in south China for characterizing emissions of IVOCs from
29 on-road vehicles. The average emission factor of IVOCs (EF_{IVOCs}) was measured to be $16.77 \pm$
30 0.89 mg km^{-1} (Average $\pm 95\%$ C.I.) for diesel and gasoline vehicles in the fleets, and based on
31 linear regression the average EF_{IVOCs} was derived to be $62.79 \pm 18.37 \text{ mg km}^{-1}$ for diesel
32 vehicles and $13.95 \pm 1.13 \text{ mg km}^{-1}$ for gasoline vehicles. The EF_{IVOCs} for diesel vehicles from
33 this study was comparable to that reported previously for non-road engines without after-
34 treatment facilities, while the EF_{IVOCs} for gasoline vehicles from this study was much higher
35 than that recently tested for a China V gasoline vehicle. IVOCs from the on-road fleets did not
36 show significant correlation with the primary organic aerosol (POA) or total non-methane
37 hydrocarbons (NMHCs) as results from previous chassis dynamometer tests. Estimated SOA
38 production from the vehicular IVOCs and VOCs surpassed the POA by a factor of ~ 2.4 , and
39 IVOCs dominated over VOCs in estimated SOA production by a factor of ~ 7 , suggesting that
40 controlling IVOCs is of greater importance to modulate traffic-related OA in urban areas. The
41 results demonstrated that although on-road gasoline vehicles have much lower EF_{IVOCs} , they
42 contribute more IVOCs than on-road diesel vehicles due to its dominance in the on-road fleets.
43 However, due to greater diesel than gasoline fuel consumption in China, emission of IVOCs

44 from diesel engines would be much larger than that from gasoline engines, signaling the
45 overwhelming contribution of IVOC emissions by non-road diesel engines in China.

46 **1 Introduction**

47 Intermediate-volatility organic compounds (IVOCs) refer to organics with effective saturated
48 concentrations ranging from 10^3 to 10^6 $\mu\text{g m}^{-3}$, roughly corresponding to the volatility range of
49 C_{12} - C_{22} normal alkanes (n-alkanes) (Donahue et al., 2006; Zhao et al., 2014). Robinson et al.
50 (2007) have demonstrated that IVOCs, as the missing secondary organic aerosol (SOA)
51 precursors in many model studies, could efficiently narrow the gap between model predicted
52 and field observed SOA. Smog chamber studies involving individual IVOCs species, like
53 higher n-alkanes and 2-ring aromatics, have confirmed their significantly higher SOA formation
54 potentials (Chan et al., 2009; Presto et al., 2010; Liu et al., 2015). In addition, recent model
55 simulations including IVOCs as SOA precursors revealed that 30% ~ 80% of ambient SOA
56 could be explained by IVOCs (Ots et al., 2016; Zhao et al., 2016; Yang et al., 2019; Lu et al.,
57 2020; Huang et al., 2020). However, due to lack of direct measurements, these model
58 simulations used the ratios of IVOCs to other species like primary organic aerosol (POA) or
59 non-methane hydrocarbons (NMHCs) to estimate IVOCs emissions.

60 Vehicular emission is an important anthropogenic source of IVOCs especially in urban
61 environments (Tkacik et al., 2014; Jathar et al., 2014; Cross et al., 2015; Zhao et al., 2015, 2016;
62 Ots et al., 2016). IVOCs could account for ~ 60% of non-methane hydrocarbons (NMHCs)
63 from diesel vehicles and 4 – 17% from gasoline vehicles, explaining a dominant portion of
64 estimated SOA mass from diesel and gasoline exhaust (Zhao et al., 2015, 2016). Previous
65 chamber simulations on SOA formation from vehicle exhaust revealed that traditional volatile
66 organic compounds (VOCs) could not explain the formed SOA, and IVOCs instead might
67 dominate the SOA productions (Deng et al., 2020; Zhang et al., 2020). In megacities like
68 London, diesel-emitted IVOCs alone could contribute ~ 30% SOA formed in ambient air (Ots

69 et al., 2016). Therefore, for the control of fine particle pollution in urban areas, it is necessary
70 to compile and upgrade emission inventories for IVOCs, and more works are needed to
71 characterize their emissions from on-road vehicles.

72 Although previous chassis dynamometer tests used limited numbers of vehicles to characterize
73 IVOCs emission (Zhao et al., 2015, 2016; Tang et al., 2021), the results obtained from the tests
74 were widely applied to recent models and emission inventories (Liu et al., 2017; Lu et al., 2018;

75 Wu et al., 2019; Huang et al., 2020). However, driving conditions significantly influence
76 vehicular IVOCs emissions (Drozd et al., 2018; Tang et al., 2021), therefore emissions of
77 IVOCs under real-world driving conditions may be quite different from that measured with
78 chassis dynamometers.~~However, driving conditions were recently found to significantly~~
79 ~~influence vehicular IVOCs emissions (Drozd et al., 2018; Tang et al., 2021), highlighting the~~
80 ~~importance of conducting on road measurements of vehicle emitted IVOCs under real world~~
81 ~~driving condition, which could further narrow the uncertainty of vehicular IVOCs estimates in~~
82 ~~models and emission inventories.~~ Tunnel test is a widely used method to characterize vehicle

83 emissions in light of its advantage in capturing real-world emissions with a large number of
84 driving vehicles. The emissions of PM_{2.5}, carbonaceous aerosols, VOCs, NO_x, and NH₃ from
85 on-road vehicles have been widely studied based on tunnel tests (Liu et al., 2014; Zhang et al.,
86 2016, 2017, 2018). However, to the best of knowledge, till present no reports are available about
87 vehicular emission factors of IVOCs through tunnel tests.

88 In China, the number of on-road vehicles reached 348 million in 2019, more than double that
89 in 2009 (<http://www.mee.gov.cn/hjzl/sthjzk/ydyhjgl/>). However, emissions of IVOCs from
90 mobile sources in China are much understudied. Only very recently, Tang et al. (2021) tested

91 emission of IVOCs from a China V light-duty gasoline vehicle. ~~For this reason,~~As IVOC
92 emission factors derived from vehicle tests in the US have been used to update China's emission
93 inventories with the inclusion of IVOCs (Liu et al., 2017)~~-,~~it is unknown whether the
94 borrowed emission factors could well reflect the vehicular emissions of IVOCs in China. On
95 the other hand, although China has made great achievements in combating air pollution in
96 recent years, fine particle pollution is still an air quality problem in many of China's cities
97 (Wang et al., 2020). As organic matters are often the most abundant components in PM_{2.5} and
98 SOA pollution is increasingly standing out with the intensified primary emission control (Guo
99 et al., 2020), understanding IVOC emissions from on-road vehicles is of great importance given
100 that vehicle-emitted IVOCs contribute greatly to urban SOA formation (Gentner et al., 2012;
101 Wu et al., 2019; Huang et al., 2020).

102 In this study, the emissions of IVOCs from on-road vehicles under real-world driving conditions
103 were characterized through tests in an urban tunnel in Guangzhou, a megacity in south China.
104 The study aims to: 1) investigate chemical compositions and volatility of IVOCs from on-road
105 driving vehicles; 2) obtain average IVOC emission factors for on-road fleet based on tests in
106 the tunnel; 3) retrieve average IVOC emission factors for gasoline- and diesel-fueled vehicles
107 by regression analysis, taking advantage of a large number of vehicles (>30,000 per day)
108 passing the tunnel; 4) compare the SOA formation potential of vehicle-emitted IVOCs to that
109 of vehicle-emitted VOCs measured in the same campaign.

110 **2. Methodology**

111 **2.1 Field sampling**

112 Sampling campaign was concurrently conducted both at the inlet and at the outlet of the
113 Zhujiang tunnel (23 °6' N, 113 °14' E), which is located in urban Guangzhou, South China (Fig.
114 S1), on three weekdays (October 14th-16th, 2019) and two weekend days (October 13th and
115 October 19th, 2019). Detailed description of the Zhujiang tunnel could be found in our previous
116 studies (Liu et al., 2014; Zhang et al., 2016, 2017, 2018). IVOCs were collected by a sorption
117 tube (Tenax TA/ Carbograph 5TD, Marks International Ltd, UK) using an automatic sampler
118 (JEC921, Jectec Science and Technology, Co., Ltd, Beijing, China). A Teflon filter was installed
119 before the tube to remove particles in the air flow. The sampling flow rate was set at 0.6 L min⁻¹
120 and hourly samples were collected from 5:00 am to 24:00 pm on each sampling day. In order
121 to compare SOA productions from IVOCs and VOCs, hourly VOCs samples were collected on
122 13th October 2019 with stainless-steel canisters at a flow rate of 66.7 mL min⁻¹ using a Model
123 910 Pressurized Canister Sampler (Xonteck, Inc., CA, USA). 2-hour quartz filter samples were
124 also collected by a high-volume PM_{2.5} sampler (Thermo Electron, Inc., USA) at the outlet and
125 inlet sampling sites from 13th October to 19th October. Trace gases were measured by online
126 analyzers (CO, Model 48i, Thermo Electron Inc., USA; NO_x, Model 42i, Thermo Electron Inc.,
127 USA). A video camera was installed at the inlet to record the vehicle flow during the campaign.

128 After sampling, the videotapes were used to count the passing vehicles and classify ~~the vehicles~~
129 into different fuel types.

130 **2.2 Laboratory analysis**

131 Sampled sorption tubes were analyzed by a thermal desorption (TD) system (TD-100, Marks
132 International Ltd, UK) coupled to a gas chromatography / mass selective detector (GC/MSD;
133 ~~Agilent~~, 7890 GC/5975 MSD, Agilent Technologies, USA) with a capillary column (~~Agilent~~,

134 HP-5MS, 30 m × 0.25 mm × 0.25 μm, [Agilent Technologies, USA](#)). Deuterated standards (C₁₂-
135 d₂₆, C₁₆-d₃₄, C₂₀-d₄₂, naphthalene-d₈, acenaphthene-d₁₀ and phenanthrene-d₁₀) were injected into
136 the sorption tubes to determine their recoveries before analysis. The sampled sorption tubes and
137 field blanks were thermally desorbed at 320 °C for 20 min, and the desorbed compounds were
138 carried by high purity helium into a cryogenic trap at -10 °C, and then the trap was rapidly
139 heated to transfer them into the GC/MSD system. The initial temperature of GC oven was set
140 at 65 °C, held for 2 min, then increased to 290 °C at 5 °C min⁻¹ and kept at 290 °C for 20 min.
141 The MSD was used in the SCAN mode with an electron impacting ionization at 70 eV.
142 Individual speciated IVOCs were quantified with the calibration curves by using authentic
143 standards. The total IVOCs mass was determined using the approach developed by Zhao et al.
144 (2014, 2015, 2016) and the detailed description was provided in the supporting information
145 (Text S1). Briefly, the total ion chromatogram (TIC) of IVOCs was divided into 11 bins based
146 on the retention times of C₁₂-C₂₂ n-alkanes. Each bin centered on the retention time of a n-
147 alkane. The start time and end time of the bin was determined by the average retention time of
148 two successive n-alkanes. For example, the start time of Bin16 (B16) was calculated as the
149 average retention time of n-C₁₅ and n-C₁₆, and the end time of B16 as the average retention time
150 of n-C₁₆ and n-C₁₇. The IVOCs mass in each bin was quantified by the response factor of n-
151 alkane in the same bin. The total IVOCs mass was the sum of IVOCs mass determined in the
152 11 bins. The mass of unresolved complex mixtures of IVOCs (UCM-IVOCs) was determined
153 by the difference between the total IVOCs and speciated IVOCs in each bin. The UCM-IVOCs
154 were further classified into unspciated branch alkanes (b-alkanes) and cyclic compounds
155 (Zhao et al., 2014)(Text S1). The analysis of VOCs can be found elsewhere (Zhang et al., 2018).

156 The POA emission was estimated as 1.2 times of organic carbon that measured in quartz filter
157 samples (Zhao et al., 2015), which were analyzed by an OC/EC analyzer (DRI Model 2015,
158 Nevada, USA) (Li et al., 2018).

159 **2.3 Quality assurance and quality control (QA/QC)**

160 Before their use for field sampling, sorption tubes were conditioned at 320 °C for 2 hours at
161 oxygen-free nitrogen flow and then sealed at both ends with brass storage caps fitted with PTFE
162 ferrules. About 15% of conditioned tubes were selected randomly to be analyzed in the same
163 way as normal samples to check if any targeted species existed in the tubes. The batch of
164 sorption tubes were certified as clean if speciated IVOCs were not found or presented in levels
165 below the method detection limits (MDLs). Before and after sampling, the flow rates of
166 samplers were calibrated by a soap-membrane flowmeter (Gilian Gilibrator-2, Sensidyne,
167 USA). During the sampling, ten field blanks (five at the inlet and five at the outlet) were
168 collected by installing a sorption tube onto the sampler each day but with pump off at both the
169 inlet and the outlet. The speciated IVOCs were not detected or presented in levels below their
170 MDLs in the blanks. MDLs for all the speciated IVOCs, including n-alkanes and polycyclic
171 aromatic hydrocarbons (PAHs), were below 8 ng m⁻³, such as 5.8 ng m⁻³ for n-C₁₂, 5.9 ng m⁻³
172 for n-C₁₆ and 4.7 ng m⁻³ for n-C₂₂. To check if any breakthrough occurred during the sampling,
173 prior to the field campaign two sorption tubes were connected in series to sample at the tunnel
174 outlet station in the same way. IVOCs detected in the second tube only accounted for 2.6 ± 1.4%
175 of the total in the two tubes, indicating negligible ~~no~~-breakthrough during the sampling. To
176 check the recoveries during thermo-desorption, selected sampled sorption tubes were analyzed
177 twice by the TD-GC/MS system, and the desorption recoveries, calculated as the percentage of

178 IVOCs in first analysis, were $96.7 \pm 3.2\%$ on average. Duplicated samples revealed less than
179 15% differences for all the speciated IVOCs.

180 **2.4 Calculation of IVOCs emission factor**

181 The vehicular EF of IVOCs can be calculated by following equation (Pierson et al., 1983; Zhang
182 et al., 2016, 2017, 2018):

$$183 \quad EF = \frac{\Delta C \times V_{air} \times T \times A}{N \times l} \quad (1)$$

184 where EF ($\text{mg km}^{-1} \text{ veh}^{-1}$) is the fleet-average emission factor of a given species during the
185 time interval T (1 h in this study); ΔC (mg m^{-3}) is the inlet-outlet incremental concentration of
186 IVOCs; V_{air} (m s^{-1}) is wind speed parallel to the tunnel measured by a 3-D sonic anemometer
187 (Campbell, Inc.); A (m^2) is the cross sectional area of the tunnel; N is the number of vehicles
188 travelling through the tunnel during the time interval T; l (km) is the distance between the outlet
189 and the inlet.

190 **3. Results and discussions**

191 **3.1 Emission factors and compositions of IVOCs**

192 Fig. 1 shows diurnal variations of vehicle numbers and vehicular IVOCs emission factors
193 (EF_{IVOCs}) during the campaign. Traffic flow in the tunnel varied 571-2263 vehicles per hour
194 during the campaign, and gasoline vehicles (GVs) dominated the vehicle fleets with a share of
195 76.3% on average, diesel vehicles (DVs) only accounted for 4.0%, and other types of vehicles,
196 including liquefied petroleum gas vehicles (LPGVs) and electrical vehicles (EVs), had an
197 average percentage of 18.7% (Fig. S2). As LPGVs and EVs are considered to have no IVOCs
198 emissions (Stewart et al., 2021), only GV and DV are responsible for the inlet-outlet

199 incremental concentrations of IVOCs. Based on above equation (1), fleet-average EF_{IVOCs} (GVs
 200 + DVs) ranged from $13.29 \pm 5.08 \text{ mg km}^{-1} \text{ veh}^{-1}$ to $21.40 \pm 5.01 \text{ mg km}^{-1} \text{ veh}^{-1}$. ~~Based on above~~
 201 ~~equation (1), average EF_{IVOCs} for GV and DVs in the vehicle fleets ranged from 13.29 ± 5.08~~
 202 ~~$\text{mg km}^{-1} \text{ veh}^{-1}$ to $21.40 \pm 5.01 \text{ mg km}^{-1} \text{ veh}^{-1}$,~~ with an average of $16.77 \pm 0.89 \text{ mg km}^{-1} \text{ veh}^{-1}$
 203 (Average $\pm 95\%$ C.I.) (Fig. 1). The average EF_{IVOCs} for DVs and GV s could be further derived
 204 through linear regression as below (Ho et al., 2007; Kramer et al., 2020):

$$205 \quad EF_{IVOCs} = EF_{DV} \times \alpha + EF_{GV} \times (1 - \alpha) \quad (2)$$

206 where EF_{IVOCs} represents the fleet-average emission factor measured during a time interval;
 207 EF_{DV} and EF_{GV} are the average EF_{IVOCs} for DVs and GV s, respectively; α is the fraction of
 208 DVs in the total IVOCs-emitting ~~diesel~~ DVs and GV s traveling through the tunnel. Based on
 209 the regression results (Fig. S3), the average EF_{IVOCs} for DVs ($62.79 \pm 18.37 \text{ mg km}^{-1} \text{ veh}^{-1}$) was
 210 ~ 4.5 times that for GV s ($13.95 \pm 1.13 \text{ mg km}^{-1} \text{ veh}^{-1}$).

211 The mileage-based EF can be converted to fuel-based EF with the fuel density and fuel
 212 efficiency (Text S2) (Zhang et al., 2016). Thus, we could obtain an average fuel-based EF_{IVOCs}
 213 of $239.5 \pm 19.5 \text{ mg kg}^{-1}$ for GV s and $984.9 \pm 288.2 \text{ mg kg}^{-1}$ for DVs. Zhao et al. (2015, 2016)
 214 measured IVOCs emissions from DVs and GV s in the US by the dynamometer tests. As shown
 215 in Fig. 2, the average EF_{IVOCs} for DVs measured in our study was significantly lower than that
 216 for DVs without any diesel particulate filter (DPF) in the US, but over 4 times higher than that
 217 with DPF. It is worth noting that the EF_{IVOCs} for DVs from this study was comparable to that
 218 for ships and non-road construction machineries (NRCMs) with diesel-fueled engines in China
 219 (Fig. 2) (Huang et al., 2018; Qi et al., 2019). As a matter of fact, China III or lower emission
 220 standard DVs accounted for $\sim 40\%$ of China's total in-use DVs in 2019

221 http://www.mee.gov.cn/xxgk/xxgk13/202012/t20201201_810776.html)-
222 <http://www.mee.gov.cn/>), and like the non-road engines, they are not equipped with any after-
223 treatment facilities. Although the after-treatment systems are installed in the China IV and
224 China V DVs, their working performance might be not so satisfactory (Wu et al., 2017). This
225 may explain why the DVs in this study had IVOCs-EFs comparable to non-road engines. The
226 EF_{IVOCs} for GVs from this study fell into the ranges of that for GVs in the US, but was at the
227 high-end of the tested values (Fig. 2). A recent study revealed a significantly lower EF_{IVOCs} of
228 83.7 mg kg^{-1} for a China V gasoline vehicle (Tang et al., 2021), implying that upgrading the
229 emission standard could help reduce emissions of IVOCs from GVs, as China IV and China III
230 GVs still share a much larger portion than the China V and VI ones in ~~China's~~ the on-road fleets
231 <http://www.mee.gov.cn/hjzl/sthjzk/ydyhjgl/201909/P020190905586230826402.pdf>)-
232 <http://www.mee.gov.cn/>).

233 Fig. 3 shows the EFs and compositions of the vehicular IVOCs in each retention-time based
234 bin (Table S1). Similar to previous studies (Zhao et al., 2015, 2016; Huang et al., 2018; Qi et
235 al., 2019; Tang et al., 2021), the unspeciated cyclic compounds dominated the IVOCs,
236 accounting for $59.07 \pm 1.06\%$, followed by unspeciated b-alkanes ($25.27 \pm 0.75\%$) and
237 speciated IVOCs ($15.66 \pm 0.60\%$). ~~The Among the~~ speciated IVOCs (Table S1), ~~consist of n-~~
238 ~~alkanes, b-alkanes and PAHs.~~ ~~N~~naphthalene dominated the quantified PAHs, accounting for
239 $56.82 \pm 1.21\%$ of total PAHs emissions. The distribution of IVOCs in retention-time based bins
240 presented a significant decreasing trend with bin numbers. Previous studies have reported that
241 more than 50% of IVOCs concentrated in higher-volatility bins like B12, B13 and B14 in
242 gasoline exhaust while much broader volatility distributions were found in diesel exhaust (Zhao

243 et al., 2015, 2016; Tang et al., 2021). The IVOCs in B12 measured in this study was also the
244 most abundant as the GVs previously tested in the US (Fig. S4). This was reasonable since the
245 GVs dominated the vehicle fleets during our tunnel experiments (Fig. S2). As shown in Fig. S5,
246 the IVOCs determined in each volatility bin well correlated with those in the volatility bins
247 close to them, and the total IVOCs have stronger correlations with IVOCs in the higher-
248 volatility bins like B12, B13 and B14. In addition, the n-alkanes, as displayed in Table S2, were
249 found to be significantly correlated to the total IVOCs that determined in the same volatility
250 bins except for B20 and n-C₂₀. The mass ratios of IVOCs ~~_in each bin~~ to the n-alkane in the
251 ~~same bins~~ ranges ranged 9.0-15.8 (Table S2). As n-alkanes can beare more easily and routinely
252 quantified, the relationships of IVOCs and n-alkanes in each volatility bin might be used to
253 estimate total IVOCs from on-road vehicles. However, vehicles types should be taken into
254 consideration when using these ratios, as the results ~~obtained~~ here were obtained forbased on a
255 fleet dominated by GVs.

256 3.2 Relationships of IVOCs with other species

257 Emissions of IVOCs from vehicles are often estimated by assuming a ratio of IVOCs to other
258 species such as POA or NMHCs (Shrivastava et al., 2008; Pye et al., 2010; Gentner et al., 2012;
259 Murphy et al., 2017; Wu et al., 2019). However, these ratios might be highly variable with fuel
260 types, operation conditions and engine performance (Lu et al., 2018). As demonstrated in Fig.
261 S6 (a) and (b), IVOCs correlated well with NO_x ($R = 0.63$, $p < 0.05$) and CO ($R = 0.58$, $p <$
262 0.05), with an average IVOCs-to-NO_x ratio of 0.039 ± 0.004 and an average IVOCs-to-CO
263 ratio of 0.033 ± 0.015 . The measured IVOCs-to-POA ratio was 3.35 ± 1.79 (Fig. S6 (c)),
264 comparable to that of 3.0 ± 0.9 for GVs previously measured in dynamometer tests simulating

265 arterial and freeway cycles, but much higher than that of 1.5 previously used for estimating
266 vehicle emissions in models (Robinson et al., 2007; Hodzic et al., 2010). As shown in Fig. S6
267 (d), the average IVOCs-to-NMHCs ratio measured in this study was 0.36 ± 0.09 , lower than
268 that previously measured for diesel vehicle exhaust (0.6 ± 0.1) (Zhao et al., 2015), but higher
269 than that previously measured for gasoline vehicle exhaust (< 0.2) (Zhao et al., 2016; Tang et
270 al., 2021). It is worth noting that the IVOCs did not present significant correlations with POA
271 or NMHCs from this study for on-road vehicle fleets (Fig. S6 (c) and (d)). This would cast
272 uncertainty over the emission estimates of IVOCs based on their ratios to POA or NMHCs.

273 3.3 Estimated SOA production from IVOCs

274 SOA formation potentials of IVOCs from on-road vehicle fleet as measured in this tunnel study
275 can be estimated as:

$$276 \quad SOA_{FP} = \sum EF_i \times Y_i \quad (3)$$

277 where SOA_{FP} is the SOA formation potential from the gaseous precursors; EF_i represents the
278 emission factor of precursor i and Y_i is the SOA yield of precursor i under high-NO_x at OA
279 concentration of $20 \mu\text{g m}^{-3}$ (Zhao et al., 2015; Huang et al., 2018; Qi et al., 2019; Tang et al.,
280 2021) (Table S3). As shown in Fig. 4, the SOA formation potentials from vehicular VOCs and
281 IVOCs totaled $8.24 \pm 0.68 \text{ mg km}^{-1}$. The SOA-to-POA ratio was 2.41 ± 1.45 , which was
282 comparable to that of GVs tested in China (1.8-4.4) (Tang et al., 2021), and that of GVs (3.6)
283 (Zhao et al., 2016) and high-speed DVs (3.2 ± 1.7) without DPF in the US (Zhao et al., 2015).
284 Our previous chamber studies simulating SOA formation from vehicles exhaust revealed the
285 SOA-to-POA ratios of 2.0 for DVs and 3.8 for GVs when cruising at 40 km h^{-1} (Deng et al.,
286 2020; Zhang et al., 2020), which is near the average driving speed of vehicles in the tunnel.

287 Among the vehicle-emitted SOA precursors, similar to previous studies (Zhao et al., 2015, 2016;
288 Huang et al., 2018; Qi et al., 2019; Tang et al., 2021), IVOCs produced significantly higher
289 SOA ($7.19 \pm 0.62 \text{ mg km}^{-1}$), ~ 7 times that from traditional VOCs ($1.04 \pm 0.30 \text{ mg km}^{-1}$).
290 Previous smog chamber studies found that SOA formed during photoaging of vehicle exhaust
291 could not be explained by traditional VOCs especially for vehicles cruising at higher speeds
292 (Robinson et al., 2007; Deng et al., 2020; Zhang et al., 2020). If this $\text{SOA}_{\text{IVOCs-to-SOA}_{\text{VOCs}}}$ ratio
293 of 7 from this study is used to re-estimate the SOA formation from exhaust for vehicles cruising
294 at 40 km h^{-1} in our previous chamber studies (Deng et al., 2020; Zhang et al., 2020), the VOCs
295 plus IVOCs precursors could explain 91% – 98% SOA formed for GVs and 31.2% – 48.2%
296 SOA formed for DVs. Zhao et al. (2015, 2016) reported significant higher $\text{SOA}_{\text{IVOCs-to-}}$
297 SOA_{VOCs} ratio for diesel vehicle exhaust than gasoline vehicle exhaust. Furthermore, we also
298 resolved the $\text{SOA}_{\text{IVOCs-to-SOA}_{\text{VOCs}}}$ ratios for DVs and GVs via liner regression (Text S3). As
299 shown in Fig. S7, although the correlation between $\text{SOA}_{\text{IVOCs-to-SOA}_{\text{VOCs}}}$ ratios and DV
300 fractions was not significant, the DVs did present much higher average $\text{SOA}_{\text{IVOCs-to-SOA}_{\text{VOCs}}}$
301 ratio (54.9) than that of GVs (6.82). Thus, $\text{SOA}_{\text{IVOCs-to-SOA}_{\text{VOCs}}}$ ratio of 7 obtained from this
302 study in a tunnel dominated by GVs would underestimate $\text{SOA}_{\text{IVOCs}}$ from DVs, consistent with
303 higher NMHCs to IVOCs ratios in gasoline exhaust than in diesel exhaust (Zhao et al., 2015,
304 2016; Huang et al., 2018; Qi et al., 2019; Tang et al., 2021). Overall, the observed vehicular
305 IVOCs as SOA precursors can help achieve mass closure between predicted and measured SOA.

306 **4. Conclusions and implications**

307 Organic aerosol (OA), primary or secondary, accounts for a large fraction of particle matters
308 (Zhang et al., 2007; Jimenez et al., 2009). On-road vehicles could be an important source of

309 OA especially in urban environment (Gentner et al., 2017). Similar to previous smog chamber
310 simulation results about SOA formed from photochemical aging of vehicle exhaust (Deng et
311 al., 2020; Zhang et al., 2020), our tunnel test also demonstrated that estimated SOA surpassed
312 the POA emission. In addition, IVOCs was found to dominate over traditional VOCs in SOA
313 formation potentials by a factor of ~ 7 , implying that reducing vehicle-emitted IVOCs is of
314 greater importance to modulate SOA for further reducing fine particle pollution particularly in
315 urban areas. As for the ratios of IVOCs to other primary species, our tunnel tests for on-road
316 fleet revealed that although the ratios of IVOCs-to-POA and IVOCs-to-NMHCs were
317 comparable to that from complex and different results when compared to that from previous
318 chassis dynamometer tests, no significant positive correlations were found between IVOCs and
319 POA or NMHCs in our tunnel measurements. This ~~implying~~ implied that cautions should be
320 taken when applying the ratios from chassis dynamometer tests to estimate real-world traffic
321 emissions, or applying the ratios in the US to estimate the emissions in China or other regions.
322 As IVOCs is not considered in normal vehicle emission tests, more field works characterizing
323 real-world vehicular emissions of IVOCs are needed to further constrain these ratios.
324 EF_{IVOCs} for the GV-dominated fleets from our tunnel test, or EF_{IVOCs} for GVs derived from
325 regression, was much higher than that from a recent chassis test for a China V gasoline vehicle
326 (Tang et al., 2021), suggesting that stricter emission standards might help reduce emissions of
327 IVOCs from GVs. Meanwhile, the EF_{IVOCs} for on-road DVs was comparable to that for non-
328 road engines without any after-treatments (Huang et al., 2018; Qi et al., 2019), suggesting that
329 facilitating the installation of after-treatment devices with stricter emission standards or

330 improving the performance of existing after-treatment devices are crucial to lower IVOC
331 emissions from DVs, which have much bigger EF_{IVOCs} than GVs.

332 Based on the regression-derived average EF_{IVOCs} for GVs and DVs and the camera-recorded
333 fleet compositions, we could estimate that ~ 81% of IVOCs by vehicles travelling through the
334 tunnel were coming from GVs and only ~ 19% were from DVs ([Table S4](#)). This is reasonable
335 since DVs have bigger EF_{IVOCs} and however much lower proportions in the fleets. These
336 percentages may underestimate the contribution to IVOCs by on-road DVs in regional or
337 national scales since DVs travel less in core urban areas due to traffic restriction rules in China.

338 Differently, in an updated emission inventory of vehicular IVOCs in China (Liu et al., 2017)
339 based on EF_{IVOCs} tested in the US, emission of IVOCs from DVs (145.07 Gg) was about 2.6
340 times that from GVs (55.30 Gg) in China in 2015. However, the ratio of DV- EF_{IVOCs} to GV-
341 EF_{IVOCs} used in the study (Liu et al., 2017) on average was much higher than that of ~ 4.5 from
342 this study for on-road vehicles. Using the EF_{IVOCs} from tests in the US might underestimate
343 IVOCs emissions from GVs but overestimate that from DVs in China. As an example, EF_{IVOCs}
344 of 83.7 mg kg⁻¹ reported very recently for a China V gasoline vehicle (Tang et al., 2021) was
345 still much higher than the maximum EF_{IVOCs} (47.15 mg kg⁻¹) they adopted for China V GVs,
346 and the EF_{IVOCs} used for China III and China IV DVs were however significantly larger than
347 that from our tunnel tests (Fig. 2) for on-road DVs (mostly China III and China IV) (Liu et al.,
348 2017). In 2019 the gasoline and diesel fuel consumptions in China were 1.20×10^2 Tg and 1.50
349 $\times 10^2$ Tg, respectively (<http://www.mee.gov.cn/hjzl/sthjzk/ydyhjgl/>). Since that gasoline is
350 mostly used for on-road vehicles while diesel may be used for both on-road and non-road
351 engines, and that EF_{IVOCs} for on-road diesels [vehicles](#) are comparable to ~~the~~ [that for](#) non-road

352 diesel engines (Huang et al., 2018; Qi et al., 2019), we could use the fuel-based EF_{IVOCs}
353 converted from our study to roughly estimate IVOCs from diesel and gasoline combustion. This
354 way estimated emission of IVOCs from diesel engines (147.74 Gg) was about 5 times that from
355 gasoline engines (28.74 Gg) in China in 2019 ([Table S4](#)). In comparison of previous study (Liu
356 et al., 2017), this result implies large uncertainties or even inconsistencies about China's
357 vehicular IVOC emission estimates. Moreover, as diesel vehicle shares less than 10% among
358 China's motor vehicles and a substantial part of diesel fuel is consumed by non-road engines,
359 the diesel-related IVOCs may largely come overwhelmingly from non-road engines instead of
360 on-road DVs, signaling the increasingly important role of non-road engines as sources of
361 IVOCs with the progress in on-road vehicles emission control.

362 **Data availability.** The dataset for this paper is available upon request from the corresponding
363 author (wangxm@gig.ac.cn)

364 **Competing interests.** The authors declare no competing financial interest.

365 **Author Contributions.** X.W. and Y.Z. designed the campaign and provided the funding
366 supports. H.F. and H.X. analyzed the samples. H.F. wrote the paper. G.Z., W.H., M.T., X.D.,
367 and X.B. provided suggestions for this paper. X.W. revised and edited the paper. The others in
368 author list conducted the field work.

369 **Acknowledgements.**

370 This work was by funded by Natural Science Foundation of China (41530641/41961144029),
371 the National Key Research and Development Program (2016YFC0202204/2017YFC0212802),
372 the Chinese Academy of Sciences (QYZDJ-SSW-DQC032), and Department of Science and
373 Technology of Guangdong Province (2017B030314057/2017BT01Z134/2019B121205006).

374 **References**

- 375 Chan, A. W. H., Kautzman, K. E., Chhabra, P. S., Surratt, J. D., Chan, M. N., Crouse, J. D.,
376 Kürten, A., Wennberg, P. O., Flagan, R. C., and Seinfeld, J. H.: Secondary organic aerosol
377 formation from photooxidation of naphthalene and alkylnaphthalenes: implications for
378 oxidation of intermediate volatility organic compounds (IVOCs). *Atmos. Chem. Phys.*, 9,
379 3049-3060, <https://doi.org/10.5194/acp-9-3049-2009>, 2009.
- 380 Cross, E. S., Sappok, A., Wong, V., and Kroll, J. H.: Load-dependent emission factors and
381 chemical characteristics of IVOCs from a medium-duty diesel engine. *Environ. Sci.*
382 *Technol.*, 49, 13483-13491, <https://doi.org/10.1021/acs.est.5b03954>, 2015.
- 383 Deng, W., Fang, Z., Wang, Z. Y., Zhu, M., Zhang, Y. L., Tang, M. J., Song, W., Lowther, S.,
384 Huang, Z. H., Jones, K., Peng, P. A., and Wang, X. M.: Primary emissions and secondary
385 organic aerosol formation from in-use diesel vehicle exhaust: comparison between idling
386 and cruise mode. *Sci. Total Environ.*, 699, 134357,
387 <https://doi.org/10.1016/j.scitotenv.2019.134357>, 2020.
- 388 Donahue, N. M., Robinson, A. L., Stanier, C. O., and Pandis, S. N.: Coupled partitioning,
389 dilution, and chemical aging of semivolatile organics. *Environ. Sci. Technol.*, 40, 2635-43,
390 <https://doi.org/10.1021/es052297c>, 2006.
- 391 Drozd, G. T., Zhao, Y. L., Saliba, G., Frodin, B., Maddox, C., Oliver Chang, M. C., Maldonado,
392 H., Sardar, S., Weber, R. J., Robinson, A. L., and Goldstein, A. H.: Detailed speciation of
393 intermediate volatility and semivolatile organic compound emissions from gasoline
394 vehicles: effects of cold-starts and implications for secondary organic aerosol formation.
395 *Environ. Sci. Technol.*, 53, 1706-1714. <https://doi.org/10.1021/acs.est.8b05600>, 2018.

396 Gentner, D. R., Isaacman, G., Worton, D. R., Chan, A. W. H., Dallmann, T. R., Davis, L., Liu,
397 S., Day, D. A., Russell, L. M., Wilson, K. R., Weber, R., Guha, A., Harley, R. A., and
398 Goldstein, A. H.: Elucidating secondary organic aerosol from diesel and gasoline vehicles
399 through detailed characterization of organic carbon emissions. *Proc. Natl. Acad. Sci. U. S.*
400 *A.*, 109, 18318–18323, <https://doi.org/10.1073/pnas.1212272109>, 2012.

401 Gentner, D. R., Jathar, S. H., Gordon, T. D., Bahreini, R., Day, D. A., El Haddad, I., Hays, P.
402 L., Pieber, S. M., Platt, S. M., de Gouw, J., Goldstein, A. H., Harley, R. A., Jimenez, J. L.,
403 Prévôt, A. S. H., and Robinson, A. L.: Review of urban secondary organic aerosol
404 formation from gasoline and diesel motor vehicle emissions. *Environ. Sci. Technol.*, 51,
405 1074-1093, <https://doi.org/10.1021/acs.est.6b04509>, 2017.

406 Guo, J. C., Zhou, S. Z., Cai, M. F., Zhao, J., Song, W., Zhao, W. X., Hu, W. W., Sun, Y. L., He,
407 Y., Yang, C. Q., Xu, X. Z., Zhang, Z. S., Cheng, P., Fan, Q., Hang, J., Fan, S. J., Wang, X.
408 M., and Wang, X. M.: Characterization of submicron particles by time-of-flight aerosol
409 chemical speciation monitor (ToF-ACSM) during wintertime: aerosol composition,
410 sources, and chemical processes in Guangzhou, China. *Atmos. Chem. Phys.*, 20, 7595-
411 7615, <https://doi.org/10.5194/acp-20-7595-2020>, 2020.

412 Hodzic, A., Jimenez, J. L., Madronich, S., Canagaratna, M. R., DeCarlo, P. F., Kleinman, L.,
413 and Fast, J.: Modeling organic aerosols in a megacity: potential contribution of semi-
414 volatile and intermediate volatility primary organic compounds to secondary organic
415 aerosol formation. *Atmos. Chem. Phys.*, 10, 5491-5514, [https://doi.org/10.5194/acp-10-](https://doi.org/10.5194/acp-10-5491-2010)
416 [5491-2010](https://doi.org/10.5194/acp-10-5491-2010), 2010.

417 Huang, C., Hu, Q. Y., Li, Y. J., Tian, J. J., Ma, Y. G., Zhao, Y. L., Feng, J. L., An, J. Y., Qiao, L.
418 P., Wang, H. L., Jing, S. A., Huang, D. D., Lou, S. R., Zhou, M., Zhu, S. H., Tao, S. K.,
419 and Li, L.: Intermediate volatility organic compound emissions from a large cargo vessel
420 operated under real-world conditions. *Environ. Sci. Technol.*, 52, 12934-12942,
421 <https://doi.org/10.1021/acs.est.8b04418>, 2018.

422 Huang, L., Wang, Q., Wang, Y. J., Emery, C., Zhu, A. S., Zhu, Y. H., Yin, S. J., Yarwood, G.,
423 Zhang, K., and Li, L.: Simulation of secondary organic aerosol over the Yangtze River
424 Delta region: the impacts from the emissions of intermediate volatility organic compounds
425 and the SOA modeling framework. *Atmos. Environ.*, 118079,
426 <https://doi.org/10.1016/j.atmosenv.2020.118079>, 2020.

427 Ho, K. F., Ho, S. S. H., Cheng, Y., Lee, S. C., and Yu, J. Z.: Real-world emission factors of
428 fifteen carbonyl compounds measured in a Hong Kong tunnel. *Atmos. Environ.*, 41, 1747-
429 1758, <https://doi.org/10.1016/j.atmosenv.2006.10.027>, 2007.

430 Jathar, S. H., Gordon, T. D., Hennigan, C. J., Pye, H. O., Pouliot, G., Adams, P. J., Donahue, N.
431 M., and Robinson, A. L.: Unspeciated organic emissions from combustion sources and
432 their influence on the secondary organic aerosol budget in the United States. *Proc. Natl.*
433 *Acad. Sci. U.S.A.*, 111, 10473-10478, <https://doi.org/10.1073/pnas.1323740111>, 2014.

434 Jimenez, J. L., Canagaratna, M. R., Donahue, N. M., Prevot, A. S. H., Zhang, Q., Kroll, J. H.,
435 DeCarlo, P. F., Allan, J. D., Coe, H., Ng, N. L., Aiken, A. C., Docherty, K. S., Ulbrich, I.
436 M., Grieshop, A. P., Robinson, A. L., Duplissy, J., Smith, J. D., Wilson, K. R., Lanz, V. A.,
437 Hueglin, C., Sun, Y. L., Tian, J., Laaksonen, A., Raatikainen, T., Rautiainen, J.,
438 Vaattovaara, P., Ehn, M., Kulmala, M., Tomlinson, J. M., Collins, D. R., Cubison, M. J.,

439 Dunlea, E. J., Huffman, J. A., Onasch, T. B., Alfarra, M. R., Williams, P. I., Bower, K.,
440 Kondo, Y., Schneider, J., Drewnick, F., Borrmann, S., Weimer, S., Demerjian, K., Salcedo,
441 D., Cottrell, L., Griffin, R., Takami, A., Miyoshi, T., Hatakeyama, S., Shimono, A., Sun,
442 J. Y., Zhang, Y. M., Dzepina, K., Kimmel, J. R., Sueper, D., Jayne, J. T., Herndon, S. C.,
443 Trimborn, A. M., Williams, L. R., Wood, E. C., Middlebrook, A. M., Kolb, C. E.,
444 Baltensperger, U., and Worsnop, D. R.: Evolution of organic aerosols in the atmosphere.
445 *Science*, 326, 1525–1529, <https://doi.org/10.1126/science.1180353>, 2009.

446 Kramer, L. J., Crilley, L. R., Adams, T. J., Ball, S. M., Pope, F. D., and Bloss, W. J.: Nitrous
447 acid (HONO) emissions under real-world driving conditions from vehicles in a UK road
448 tunnel. *Atmos. Chem. Phys.*, 20, 5231-5248, <https://doi.org/10.5194/acp-20-5231-2020>,
449 2020.

450 Li, S., Zhu, M., Yang, W. Q., Tang, M. J., Huang, X. L., Yu, Y. G., Fang, H., Yu, X., Yu, Q. Q.,
451 Fu, X. X.; Song, W., Zhang, Y. L., Bi, X. H., and Wang, X. M.: Filter-based measurement
452 of light absorption by brown carbon in PM_{2.5} in a megacity in South China. *Sci. Total*
453 *Environ.*, 633, 1360-1369, <https://doi.org/10.1016/j.scitotenv.2018.03.235>, 2018.

454 Liu, H., Man, H. Y., Cui, H. Y., Wang, Y. J., Deng, F. Y., Wang, Y., Yang, X. F., Xiao, Q., Zhang,
455 Q., Ding, Y., and He, K. B.: An updated emission inventory of vehicular VOCs and IVOCs
456 in China. *Atmos. Chem. Phys.*, 17, 12709-12724, [https://doi.org/10.5194/acp-17-12709-](https://doi.org/10.5194/acp-17-12709-2017)
457 2017, 2017.

458 Liu, T. Y., Wang, X. M., Wang, B. G., Ding, X., Deng, W., Lü S. J., and Zhang, Y. L.: Emission
459 factor of ammonia (NH₃) from on-road vehicles in China: tunnel tests in urban Guangzhou.
460 *Environ. Res. Lett.*, 9, 064027, <https://doi.org/10.1088/1748-9326/9/6/064027>, 2014.

461 Liu, T. Y., Wang, X. M., Deng, W., Hu, Q. H., Ding, X., Zhang, Y. L., He, Q. F., Zhang, Z., Lü,
462 S. J., Bi, X. H., Chen, J. M., and Yu, J. Z.: Secondary organic aerosol formation from
463 photochemical aging of light-duty gasoline vehicle exhausts in a smog chamber. *Atmos.*
464 *Chem. Phys.*, 15, 9049-9062, <https://doi.org/10.5194/acp-15-9049-2015>, 2015.

465 Lu, Q., Murphy, B. N., Qin, M., Adams, P. J., Zhao, Y. L., Pye, H. O. T., Efstathiou, C., Allen,
466 C., and Robinson, A. L.: Simulation of organic aerosol formation during the CalNex study:
467 updated mobile emissions and secondary organic aerosol parameterization for
468 intermediate-volatility organic compounds. *Atmos. Chem. Phys.*, 20, 4313-4332,
469 <https://doi.org/10.5194/acp-20-4313-2020>, 2020.

470 Lu, Q., Zhao, Y. L., and Robinson, A. L.: Comprehensive organic emission profiles for gasoline,
471 diesel and gas-turbine engines including intermediate and semi-volatile organic compound
472 emissions. *Atmos. Chem. Phys.*, 18, 17637-17654, [https://doi.org/10.5194/acp-18-17637-](https://doi.org/10.5194/acp-18-17637-2018)
473 2018, 2018.

474 Murphy, B. N., Woody, M. C., Jimenez, J. L., Carlton, A. M. G., and Pye, H. O. T.: Semivolatile
475 POA and parameterized total combustion SOA in CMAQv5.2: impacts on source strength
476 and partitioning, *Atmos. Chem. Phys.*, 17, 11107-11133, [https://doi.org/10.5194/acp-17-](https://doi.org/10.5194/acp-17-11107-2017)
477 11107-2017, 2017.

478 Ots, R., Young, D. E., Vieno, M.; Xu, L., Dunmore, R. E., Allan, J. D., Coe, H., Williams, L.
479 R., Herndon, S. C., and Ng, N. L.: Simulating secondary organic aerosol from missing
480 diesel-related intermediate-volatility organic compound emissions during the clean air for
481 London (ClearfLo) campaign. *Atmos. Chem. Phys.*, 16, 1-36, [https://doi.org/10.5194/acp-](https://doi.org/10.5194/acp-16-6453-2016)
482 16-6453-2016, 2016.

483 Pye, H. O. T., and Seinfeld, J. H.: A global perspective on aerosol from low-volatility organic
484 compounds. *Atmos. Chem. Phys.*, 10, 4377–4401, [https://doi.org/10.5194/acp-10-4377-](https://doi.org/10.5194/acp-10-4377-2010)
485 2010, 2010.

486 Pierson, W. R., and Brachaczek, W. W.: Emissions of ammonia and amines from vehicles in the
487 road. *Environ. Sci. Technol.*, 17, 757-760, <https://doi.org/10.1021/es00118a013>, 1983.

488 Presto, A. A., and Miracolo, M. A.: Secondary organic aerosol formation from high-NO_x photo-
489 oxidation of low volatility precursors:n-alkanes. *Environ. Sci. Technol.*, 44, 2029-2034,
490 <https://doi.org/10.1021/es903712r>, 2010.

491 Qi, L. J., Liu, H., Shen, X. E., Fu, M. L., Huang, F. F., Man, H. Y., Deng, F. Y., Shaikh, A. A.,
492 Wang, X. T., Dong, R., Song, C., and He, K. B.: Intermediate-volatility organic compound
493 emissions from nonroad construction machinery under different operation modes. *Environ.*
494 *Sci. Technol.*, 53, 13832-13840, <https://doi.org/10.1021/acs.est.9b01316>, 2019.

495 Robinson, A. L., Donahue, N. M., Shrivastava, M. K., Weitkamp, E. A., Sage, A. M., Grieshop,
496 A. P., Lane, T. E., Pierce, J. R., and Pandis, S. N.: Rethinking organic aerosols: semivolatile
497 emissions and photochemical aging. *Science*, 315, 1259-1262,
498 <https://doi.org/10.1126/science.1133061>, 2007.

499 Shrivastava, M. K., Lane, T. E., Donahue, N. M., Pandis, S. N., and Robinson, A. L.: Effects of
500 gas particle partitioning and aging of primary emissions on urban and regional organic
501 aerosol concentrations. *J. Geophys. Res. Atmos.*, 113, D18301, [https://doi.org/](https://doi.org/10.1029/2007jd009735)
502 [10.1029/2007jd009735](https://doi.org/10.1029/2007jd009735), 2008.

503 Stewart, G. J., Nelson, B. S., Acton, W. J. F., Vaughan, A. R., Farren, N. J., Hopkins, J. R., Ward,
504 M. W., Swift, S. J., Arya, R., Mondal, A., Jangirh, R., Ahlawat, S., Yadav, L., Sharma, S.

505 K., Yunus, S. S. M., Hewitt, C. N., Nemitz, E., Mullinger, N., Gadi, R., Sahu, L. K.,
506 Tripathi, N., Rickard, A. R., Lee, J. D., Mandal, T. K., and Hamilton, J. F.: Emissions of
507 intermediate-volatility and semi-volatile organic compounds from domestic fuels used in
508 Delhi, India. *Atmos. Chem. Phys.*, 21, 2407-2426, [https://doi.org/10.5194/acp-21-2407-](https://doi.org/10.5194/acp-21-2407-2021)
509 2021, 2021.

510 Tang, R. Z., Lu, Q. Y., Guo, S., Wang, H., Song, K., Yu, Y., Tan, R., Liu, K. F., Shen, R. Z.,
511 Chen, S. Y., Zeng, L. M., Jorga, S. D., Zhang, Z., Zhang, W. B., Shuai, S. J., and Robinson,
512 A. L.: Measurement report: distinct emissions and volatility distribution of intermediate
513 volatility organic compounds from on-road chinese gasoline vehicle: implication of high
514 secondary organic aerosol formation potential. *Atmos. Chem. Phys.*, 21, 2569-2583,
515 <https://doi.org/10.5194/acp-21-2569-2021>, 2021.

516 Tkacik, D. S., Lambe, A. T., Jathar, S., Li, X., Presto, A. A., Zhao, Y. L., Blake, D., Meinardi,
517 S., Jayne, J. T., Croteau, P. L., and Robinson, A. L.: Secondary organic aerosol formation
518 from in-use motor vehicle emissions using a potential aerosol mass reactor. *Environ. Sci.*
519 *Technol.*, 48, 11235-11242, <https://doi.org/10.1021/es502239v>, 2014.

520 Wang, Y. H., Gao, W. K., Wang, S., Song, T., Gong, Z. Y., Ji, D. S., Wang, L. L., Liu, Z. R.,
521 Tang, G. Q., Huo, Y. F., Tian, S. L., Li, J. Y., Li, M. G., Yang, Y., Chu, B. W., Petaja, T. K.,
522 Kerminen, V-M., He, H., Hao, J. M., Kulmala, M., Wang, Y. S., and Zhang, Y. H.:
523 Contrasting trends of PM_{2.5} and surface-ozone concentrations in China from 2013 to 2017.
524 *Nat. Sci. Rev.*, 7, 1331-1339, <https://doi.org/10.1093/nsr/nwaa032>, 2020.

525 Wu, L. Q., Wang, X. M., Lu, S. H., Shao, M., and Ling, Z. H: Emission inventory of semi-
526 volatile and intermediate-volatility organic compounds and their effects on secondary

527 organic aerosol over the Pearl River Delta region, *Atmos. Chem. Phys.*, 19, 8141-8161,
528 <https://doi.org/10.5194/acp-19-8141-2019>, 2019.

529 Wu, Y., Zhang, S. J., Hao, J. M., Liu, H., Wu, X. M., Hu, J. N., Walsh, M. P., Wallington, T. J.,
530 Zhang, M. K., and Stevanovic, S.: On-road vehicle emissions and their control in China:
531 a review and outlook. *Sci. Total Environ.*, 574, 332-349,
532 <https://doi.org/10.1016/j.scitotenv.2016.09.040>, 2017.

533 Yang, W. Y., Li, J., Wang, W. G., Li, J. L., Ge, M. F., Sun, Y. L., Chen, X. S., Ge, B. Z., Tong,
534 S. R., Wang, Q. Q., and Wang, Z. F.: Investigating secondary organic aerosol formation
535 pathways in China during 2014. *Atmos. Environ.*, 213, 133-147,
536 <https://doi.org/10.1016/j.atmosenv.2019.05.057>, 2019.

537 Zhang, Q., Jimenez, J. L., Canagaratna, M. R., Allan, J. D., Coe, H., Ulbrich, I., Alfarra, M. R.,
538 Takami, A., Middlebrook, A. M., and Sun, Y. L.: Ubiquity and dominance of oxygenated
539 species in organic aerosols in anthropogenically-influenced northern hemisphere
540 midlatitudes. *Geophys. Res. Lett.*, 34, L13801, <https://doi.org/10.1029/2007GL029979>,
541 2007.

542 Zhang, Y. L., Wang, X. M., Wen, S., Herrmann, H., Yang, W. Q., Huang, X. Y., Zhang, Z.,
543 Huang, Z. H., He, Q.F., and George, C.: On-road vehicle emissions of glyoxal and
544 methylglyoxal from tunnel tests in urban Guangzhou, China. *Atmos. Environ.*, 127, 55-60,
545 <https://doi.org/10.1016/j.atmosenv.2015.12.017>, 2016.

546 Zhang, Y. L., Yang, W. Q., Huang, Z. H., Liu, D., Simpson, I., Blake, D. R., George, C., and
547 Wang, X. M.: Leakage rates of refrigerants CFC-12, HCFC-22, and HFC-134a from
548 operating mobile air conditioning systems in Guangzhou, China: tests inside a busy urban

549 tunnel under hot and humid weather conditions. *Environ. Sci. Technol. Lett.*, 4, 481-486,
550 <https://doi.org/10.1021/acs.estlett.7b00445>, 2017.

551 Zhang, Y. L., Yang, W. Q., Simpson, I., Huang, X. Y., Yu, J. Z., Huang, Z. H., Wang, Z. Y.,
552 Zhang, Z., Liu, D., Huang, Z. Z., Wang, Y. J., Pei, C. L., Shao, M., Blake, D. R., Zheng, J.
553 Y., Huang, Z. J., and Wang, X. M.: Decadal changes in emissions of volatile organic
554 compounds (VOCs) from on-road vehicles with intensified automobile pollution control:
555 case study in a busy urban tunnel in South China. *Environ. Pollut.*, 233, 806-819,
556 <https://doi.org/10.1016/j.envpol.2017.10.133>, 2018.

557 Zhang, Y. L., Deng, W., Hu, Q. H., Wu, Z. F., Yang, W. Q., Zhang, H. N., Wang, Z. Y., Fang,
558 Z., Zhu, M., Li, S., Song, W., Ding, X., and Wang, X. M.: Comparison between idling and
559 cruising gasoline vehicles in primary emissions and secondary organic aerosol formation
560 during photochemical ageing. *Sci. Total Environ.*, 772, 137934,
561 <https://doi.org/10.1016/j.scitotenv.2020.137934>, 2020.

562 Zhao, Y. L., Hennigan, C. J., May, A. A., Tkacik, D. S., de Gouw, J. A., Gilman, J. B., Kuster,
563 W. C., Borbon, A., and Robinson, A. L.: Intermediate-volatility organic compounds: a
564 large source of secondary organic aerosol. *Environ. Sci. Technol.*, 48, 13743-13750,
565 <https://doi.org/10.1021/es5035188>, 2014.

566 Zhao, Y. L., Nguyen, N. T., Presto, A. A., Hennigan, C. J., May, A. A., and Robinson, A. L.:
567 Intermediate volatility organic compound emissions from on-road diesel Vehicles:
568 chemical composition, emission factors, and estimated secondary organic aerosol
569 production. *Environ. Sci. Technol.*, 49, 11516-11526,
570 <https://doi.org/10.1021/acs.est.5b02841>, 2015.

571 Zhao, Y. L., Nguyen, N. T., Presto, A. A., Hennigan, C. J., May, A. A., and Robinson, A. L.:
572 Intermediate volatility organic compound emissions from on-road gasoline vehicles and
573 small off-road gasoline engines. *Environ. Sci. Technol.*, 50, 4554-4563,
574 <https://doi.org/10.1021/acs.est.5b06247>, 2016.

575

576 **Figure captions**

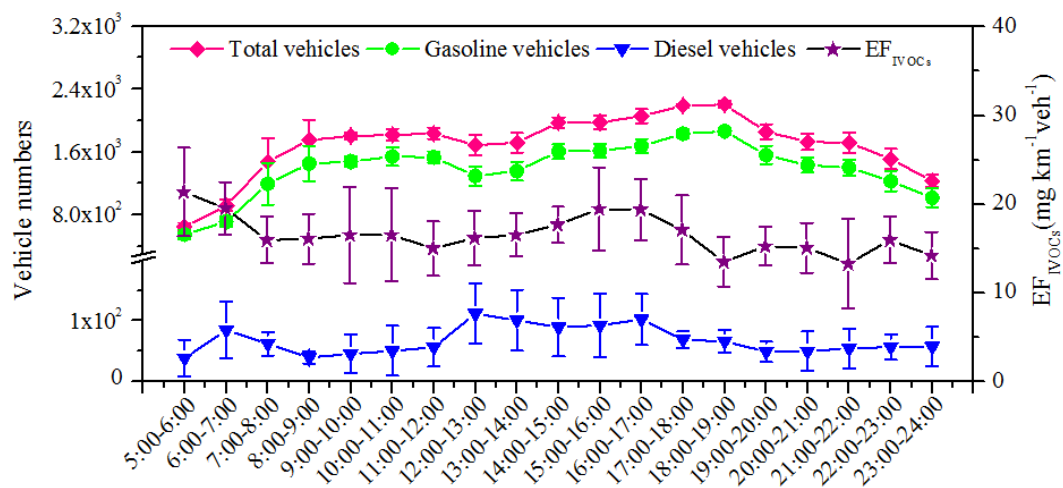
577 Figure 1. Diurnal variations of vehicle fleets and fleet-average EF_{IVOCs} during the sampling
578 period. Error bars represent 95% confidence intervals.

579 Figure 2. Comparison of the EF_{IVOCs} measured in this study with that previously measured for
580 fossil fuel combustion sources. The error bars in (a) represent 95% confidence
581 interval. In (b), the boxes represent the 75th and 25th percentiles, the centerlines are
582 the medians and squares are the averages. The whiskers represent 10th and 90th
583 percentiles. SORMs refer to small off-road engines fueled with gasoline. NRCMs
584 represent non-road construction machineries fueled with diesel.

585 Figure 3. The average emission factor of vehicular IVOCs in different bins measured during
586 the campaign.

587 Figure 4. The predicted SOA formation potentials from different classes of precursors (VOC
588 and IVOCs). The error bars represent 95% confidence intervals.

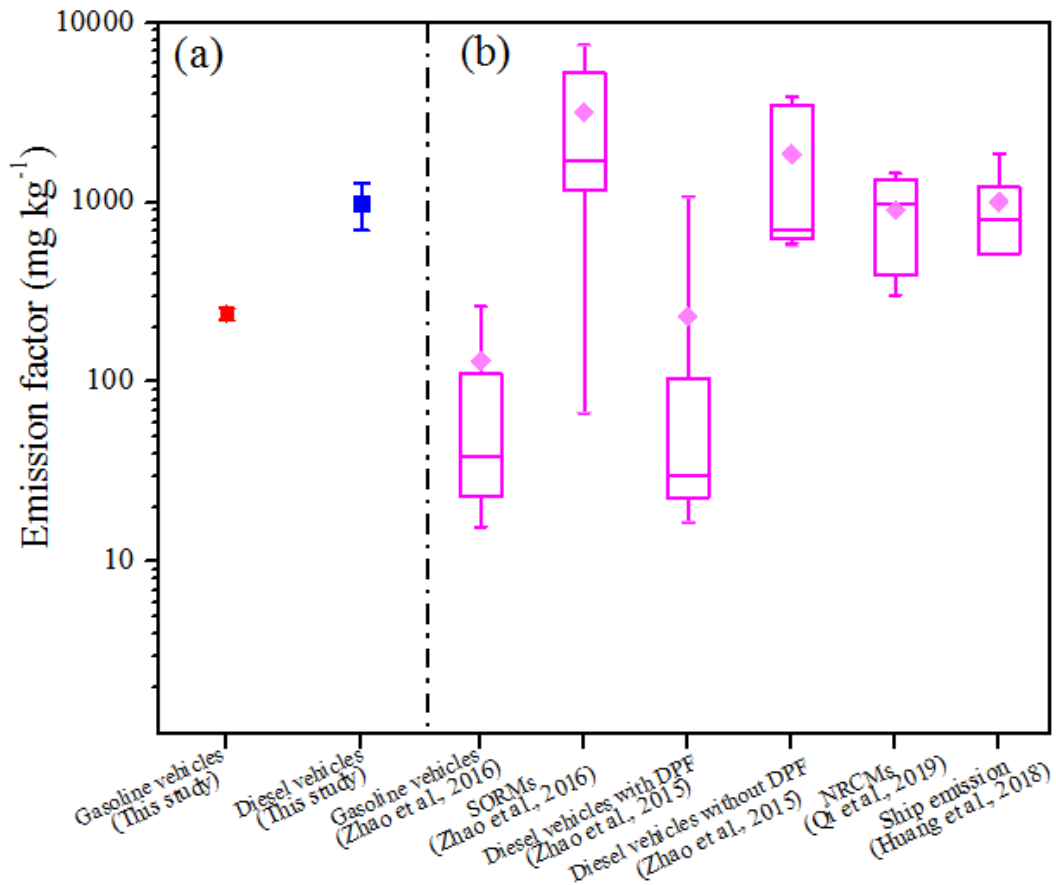
589



590

591 Figure 1. Diurnal variations of vehicle fleets and fleet-average EF_{IVOCs} during the sampling

592 period. Error bars represent 95% confidence intervals.



593

594 Figure 2. Comparison of the EF_{VOCs} measured in this study with that previously measured for

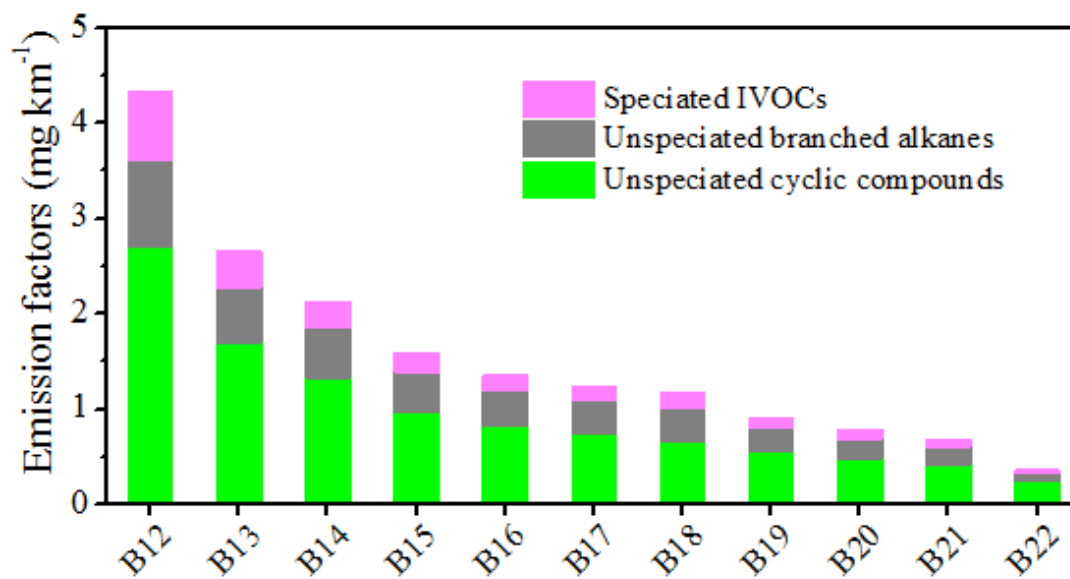
595 fossil fuel combustion sources. The error bars in (a) represent 95% confidence interval. In (b),

596 the boxes represent the 75th and 25th percentiles, the centerlines are the medians and squares are

597 the averages. The whiskers represent 10th and 90th percentiles. SORMs refer to small off-road

598 engines fueled with gasoline. NRCMs represent non-road construction machineries fueled with

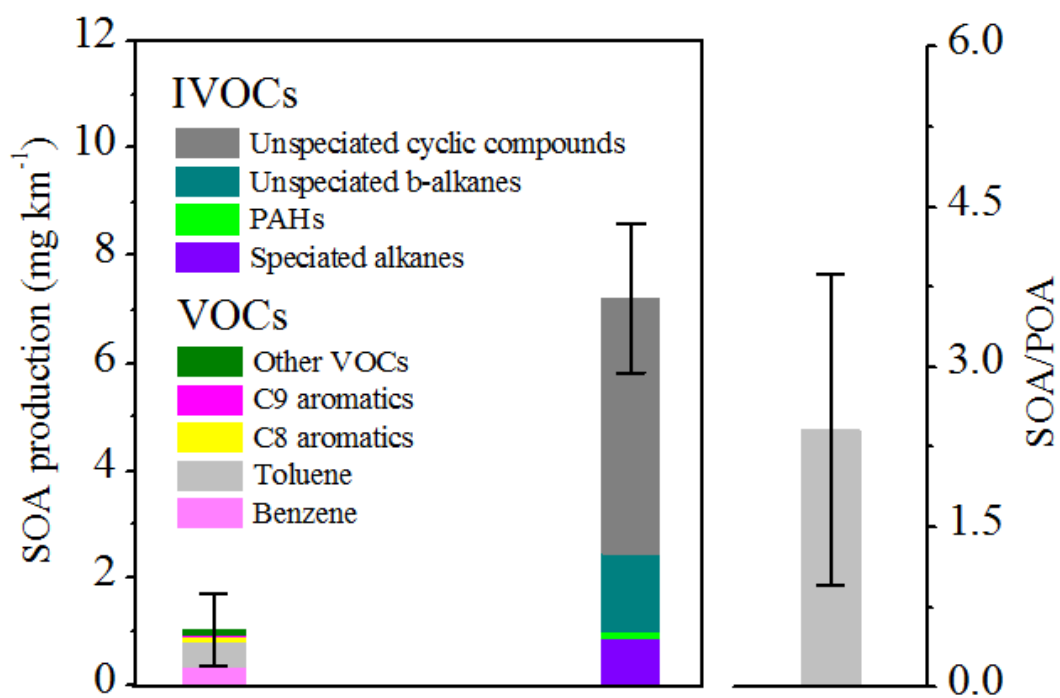
599 diesel.



600

601 Figure 3. The average emission factor of vehicular IVOCs in different bins measured during

602 the campaign.



603

604 Figure 4. The predicted SOA formation potentials from different classes of precursors (VOC

605 and IVOCs). The error bars represent 95% confidence intervals.